Catalysis Today 149 (2010) 132–137

Contents lists available at ScienceDirect

Catalysis Today

journal homepage: www.elsevier.com/locate/cattod

Synthesis and characterization of NTS material and its oxidation desulfurization properties

Chunfeng Shi *, Bin Zhu, Min Lin, Jun Long

State Key Laboratory of Catalytic Material and Reaction Engineering, Research Institute of Petroleum Processing, SINOPEC, 18 Xueyuan Road, Haidian District, Beijing 100083, China

ARTICLE INFO

Article history:
Available online 6 December 2009

Keywords:
Titanium silicalite
Noble-metal
Characterization
Hydrogen peroxide
Bi-functional catalyst

ABSTRACT

The development of desulfurization technology involving the onsite direct generation of hydrogen peroxide (H_2O_2) from $H_2 + O_2$, followed by H_2O_2 oxidation to organic oxides without conventional refining is regarded as one promising approach for reducing capital and operating costs. The objective of our research is to provide bi-functional catalytic materials based on a combined process for the oxidative desulfurization (ODS) using H_2O_2 in situ generated. We have prepared a series of new bi-functional titanosilicate (NTS, titanium silicalite combined with noble-metal loading), which have been synthesized by combining noble-metal sources with modified titanium silicalite under basic conditions. Here, the synthesis and characterization of NTS samples, and their ODS properties are presented. The samples were characterized by various analytical techniques, and their direct ODS performances were investigated. The results indicate that NTS shows well ordered MFI topology and with hollow structure; NTS combined with noble-metal shows potential for application in direct ODS with $H_2 + O_2$ in one-step process.

© 2009 Elsevier B.V. All rights reserved.

1. Introduction

The sulfur content in motor and diesel fuels is being continuously regulated to lower levels. The current method for sulfur removal in industries is mainly hydrodesulfurization (HDS), which requires high temperature and pressure, making HDS a very costly option for deep desulfurization. Moreover, it is difficult and costly to use the existing HDS technology to reduce the sulfur in fuels to less than 10 ppm, and it is also not very effective for removing heterocyclic sulfur compounds such as dibenzothiophene (DBT) and its alkyl-substituted derivatives especially 4,6-dimethyldibenzothiophene (4,6-DMDBT). In order to meet the need of ultra-clean fuels for environmental protection, it is necessary to explore new approaches to ultra-deep desulfurization of fuels [1,2].

There are many research and development efforts on alternative methods to eliminate these refractory sulfur compounds from fuels, such as selective adsorption, alkylation, reactive desorption, bio-desulfurization, oxidation/extraction or adsorption (oxidative desulfurization, ODS), etc. [1–8]. The development and application of ODS are considered to be one of the most desired options, because ODS can lower the sulfur contents under mild conditions [1,9]. The oxidant frequently used in ODS is hydrogen peroxide (H_2O_2), which is an environmentally friendly oxidant, but its manufacture is complex, expensive and energy-intensive. Attempts have already been made to directly generate H_2O_2 in situ from $H_2 + O_2$, to replace the current process since it is the most atom-efficient method to synthesize H_2O_2. The key issue of above direct oxidation technology is the design and preparation of the bi-functional catalysts. Metals such as platinum, palladium, and gold, supported on titanosilicate or other porous materials have been explored as catalysts [10,11]. The strategy is to synthesize H_2O_2 on noble-metal in situ and use it in oxidative reaction on titanosilicate. The main problem in this process is how to synthesize H_2O_2 efficiently, rendering the process economically viable [12,13]. So the issue for developing the process is improving the synthesis efficiencies of H_2O_2, by preparing new catalysts or improving the catalysts. As far as we know, the combined process is mostly applied in the epoxidation of propylene to propylene oxide [13], but the direct ODS approach using H_2O_2 in situ generated still have not been explored up to the present. In addition, the combined process also needs further research, especially in the area of designing the appropriate bi-functional catalysts.

In this paper, we present the synthesis and characterization of noble-metal titanium silicate (NTS) in basic conditions. The characterizations include X-ray fluorescence analysis (XRF), scanning electron microscopy (SEM), transmission electron microscopy (TEM), powder X-ray diffraction (XRD), N_2 adsorption isotherms (BET surface area and pore volume), Fourier transform infrared spectrometry (FT-IR), solid-state ^{29}Si magic angle spinning

* Corresponding author. Tel.: +86 10 82368754/82368801; fax: +86 10 62311290.
E-mail addresses: chfshi@yahoo.com.cn, shicf@ripp-sinopec.com (C. Shi).

0920-5861/$ – see front matter © 2009 Elsevier B.V. All rights reserved.
doi:10.1016/j.cattod.2009.11.004

nuclear magnetic resonance spectra (^{29}Si MAS NMR), ultraviolet–visible diffuse reflectance spectroscopy (UV–vis DRS), and X-ray photoelectron spectroscopy (XPS). Their catalytic direct ODS performances in the oxidation of thiophene were also investigated.

2. Experimental

2.1. Materials

Tetraethyl orthosilicate (TEOS), tetrabutyl orthotitanate (titanium butoxide, TBOT), tetrapropylammonium hydroxide (TPAOH, 25 wt% in H_2O), hydrazine hydrate ($N_2H_4{\cdot}H_2O$, 85 wt% in H_2O), hexadecyltrimethyl ammonium bromide (CTAB), methanol, triethanolamine, isopropanol, hydrochloric acid (HCl, 36 wt% in H_2O), ammonia ($NH_3{\cdot}H_2O$, 30 wt% in H_2O), palladium nitrate [$Pd(NO_3)_2$], hydrogen peroxide (H_2O_2, 30 wt% in H_2O), thiophene, methanol, n-octane were of analytical grade and purchased from Beijing Chemical Co. (China).

2.2. Synthesis

The modified titanium silicalite (modified TS-1) with hollow structure was synthesized according to the procedure similar to that described by Lin et al. [14]. One typical synthesis procedure of modified TS-1 was as follows: (1) 25.0 g of TEOS was thoroughly mixed with 8.0 g of TPAOH solution and 60.0 g of distilled water. After hydrolyzing at 70 °C for 1 h, a solution composed of 2.0 g of TBOT and 10.0 g of anhydrous isopropanol was added slowly with stirring. The mixture obtained was stirred at 65 °C for 3 h and transferred to a stainless steel autoclave and heated under autogenous pressure at 170 °C for 2 days, thereafter the mixture was filtered, washed with distilled water, dried at 100 °C for 2 h, and then calcined at 550 °C in air for 6 h; thus the TS-1 was obtained. (2) The TS-1 obtained in step 1 was mixed with a HCl solution in a ratio of TS-1 (g):HCl (mol):water (mol) = 100:0.5:150. Then, the mixture was reacted at 65 °C for 10 h. After filtration followed by washing and drying by routine methods, above acid-treated TS-1 was mixed with triethanolamine, TPAOH and water in a ratio of TS-1 (g):triethanolamine (mol):TPAOH (mol):water (mol) = 100:0.1:0.2:200, then the mixture was transferred to a stainless steel autoclave and heated at 120 °C for 12 h. After cooling and pressure release, routine filtration, washing, drying and calcination, the modified TS-1 was obtained.

Pd was supported on modified TS-1 by suspending 15 g modified TS-1 in 40 g deionized water in which 5 mL $NH_3{\cdot}H_2O$, and 0.2 g CTAB along with the appropriate amount of $N_2H_4{\cdot}H_2O$ and $Pd(NO_3)_2$ were added to the solution. The mixture was stirred for 24 h at 30 °C, and then recovered by evaporating the solvent under vacuum at 30 °C, dried at 120 °C for 24 h. Reduction was carried out with pure N_2 at a heating rate of 2 K/min from room temperature to 150 °C. Under such atmosphere, the catalysts were auto-reduced by the thermal decomposition of NH_3 ligands [13]. As determined by XRF analysis, the resulting NTS samples were loaded with 0.31 and 0.83 wt% Pd (oxide form), respectively.

2.3. Characterization

The Pd contents in NTS samples were determined by the X-ray fluorescence analysis (XRF) using Rigaku 3271E X-ray fluorescence spectrometer with semi-quantitative analysis. Scanning electron microscopy (SEM) images were collected on PHILIPS XL 30 ESEM with an acceleration voltage of 200 kV. Transmission electron microscopy (TEM) experiments were performed on a Tecnai G^2F20S-TWIN electron microscope with an acceleration voltage of 300 kV. Powder X-ray diffraction (XRD) patterns were recorded on a Siemens D5005 (30 kV, 30 mA) using nickel-filtered Cu $K\alpha$ radiation with wavelength of 0.15418 nm, diffraction patterns were collected under ambient conditions in the 2θ range of 4–40°. The nitrogen isotherms at the temperature of liquid nitrogen were measured using a Micromeritics ASAP 2010M system, the samples were outgassed for 10 h at 300 °C before measurements, the volume of adsorbed N_2 was normalized to standard temperature and pressure, specific surface areas were determined from the linear part of the BET equation. Fourier transform infrared spectra (FT-IR) were recorded on Nicolet 8210 infrared spectrometer in the range 400–4000 cm^{-1}. ^{29}Si solid-state Nuclear Magnetic Resonance (NMR) experiments were performed with magic angle spinning (MAS) on an Infinity Plus-400 spectrometer. The diffuse reflectance ultraviolet–visible (UV–vis) spectra for powder samples were obtained on a spectrometer Perkin–Elmer Lambda 20 UV-Visible spectrometer equipped with an integrating sphere. X-ray photoelectron spectra (XPS) were recorded on PHI Quantera SXM (Scanning X-ray Microprobe), in vacuum (6.7×10^{-8} Pa) at ambient temperature.

2.4. Catalytic test

Catalytic tests were performed in a 250 mL stainless steel autoclave lined with a Teflon beaker. 0.5 g catalyst, 0.05 mL thiophene, 5 mL methanol, and 45 mL n-octane were charged to the reactor. After air was removed by purging with N_2, the vessel was continuously pressurized with H_2 and O_2 (mole ratio is 1:1) until the pressure up to 2.0 MPa. The slurry was heated from room temperature to 40 °C under pressure and vigorous stirring. The reactor was kept at 40 °C for 2 and 6 h, and then cooled down to below 10 °C. At the end of reaction, the catalyst was filtered off, and the liquid phase analysis was performed on an Agilent 6890N gas chromatograph (GC), using a flame ionization detector (FID) and a 30 m fused silica capillary column (HP-FFAP, 100% polyethylene glycol TPA). Oxidation products were identified through gas chromatography–mass spectrometry (GC–MS) analysis. Here, the thiophene conversion (activity) and the mole ratio of sulfoxide to sulfone (selectivity) were used to describe their catalytic ODS performances.

3. Results and discussion

3.1. X-ray fluorescence

XRF analysis results of modified TS-1, NTS-1 and NTS-2 are listed in Table 1. It can be seen that modified TS-1 consists of SiO_2 and TiO_2, while NTS-1 and NTS-2 are composed of PdO, SiO_2 and TiO_2. With the introduction of Pd into NTS samples, their SiO_2 and TiO_2 contents decreased slightly, and the decrease in SiO_2 and TiO_2 contents match exactly with what would be expected given the presence of 0.31 and 0.83 wt% PdO in NTS-1 and NTS-2, respectively. Moreover, there are almost no changes in the ratio of TiO_2/SiO_2 for NTS samples, demonstrating that the combination of noble-metal with modified TS-1 has no severe effects on its composition.

3.2. Scanning electron microscopy

SEM micrographs of NTS-1, NTS-2 and modified TS-1 are shown in Fig. 1. The particles of all samples are uniform with the average crystal size of 0.3–0.4 μm (300–400 nm) and the typical morphology of strawberry. There are no significant differences in the morphology and particle size between modified TS-1 and NTS, indicating that the combination of noble-metal with modified TS-1 does not influence the morphology and particle size of titanium silicate. These results are in accord with the following TEM characterization.

Table 1
XRF results, porous parameters, relative crystallinity, I_{960}/I_{550} values and ODS performance of samples.

Samples	PdO (wt%)	TiO_2 (wt%)	SiO_2 (wt%)	Relative crystallinity (%)	BET surface area (m^2/g)[a]	Pore volume (cm^3/g)[b]	I_{960}/I_{550}	ODS performance			
								Thiophene conversion (%)		Selectivity sulfoxide/sulfone	
								2 h	6 h	2 h	6 h
Pd	100[c]	–	–	–	3	–	–	–	–	–	–
TS-1	–	6.25	93.75	98	412	0.25	0.692	–	–	–	–
Modified TS-1	–	6.24	93.76	100	420	0.36	0.712	–	–	–	–
NTS-1	0.31	6.19	93.50	98	405	0.34	0.701	36	75	1.4	0.7
NTS-2	0.83	6.13	93.04	95	388	0.31	0.688	52	87	1.7	0.6
Pd/TS-1[d]	0.34	6.18	93.48	91	375	0.21	0.663	12	23	2.0	1.2
Pd/MTS-1[e]	0.33	6.16	93.51	93	391	0.29	0.672	19	28	1.8	1.1

[a] Total surface area.
[b] Total pore volume.
[c] Calculated result.
[d] TS-1 impregnated with Pd.
[e] Modified TS-1 impregnated with Pd.

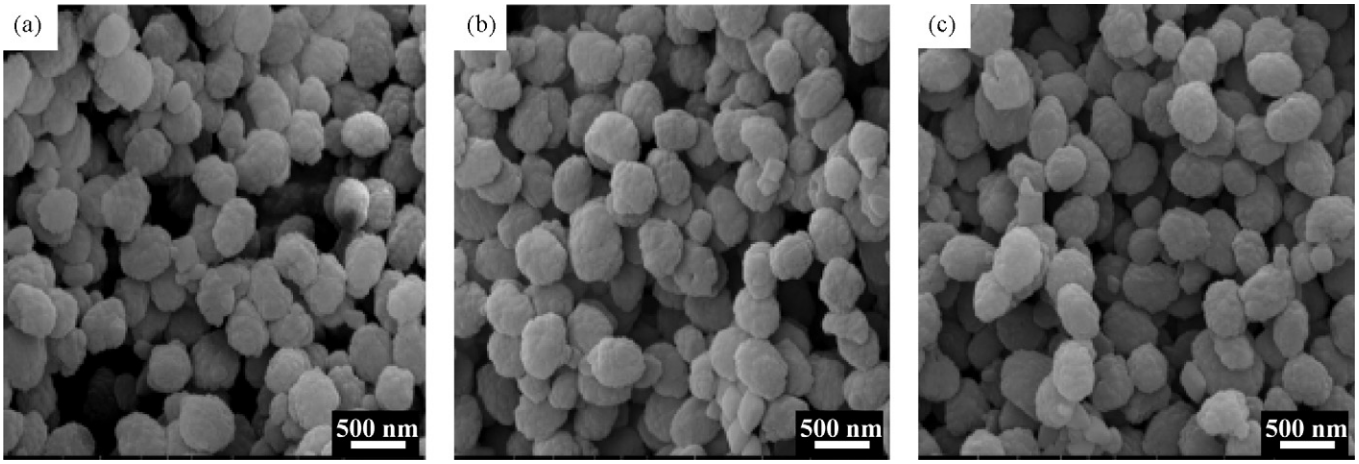

Fig. 1. SEM images of samples: (a) modified TS-1, (b) NTS-1 and (c) NTS-2.

3.3. Transmission electron microscopy

TEM experiments were used to obtain information about texture (mainly particle size, shape or morphology) and dispersion of Pd nano-particles in NTS materials. Representative TEM micrographs of samples are shown in Fig. 2, the particles of NTS-1 and NTS-2 are highly crystalline with an average crystal size of 0.3–0.4 μm, and very similar to that of SEM analysis. As illustrated in Fig. 2, the majority of particles of NTS-1, NTS-2 and modified TS-1 all show hollow structure (having intra-crystalline voids), while that of fresh TS-1 (other than modified TS-1) with solid one (not shown here) [14,20,21]. Furthermore, there are no obvious characteristic nano-particles of pure Pd in the TEM images of NTS-1 and NTS-2 (Fig. 2b and c), indicating the high dispersion of Pd in titanium silicate matrix [22,23], which are consistent with the following XRD analysis.

3.4. X-ray diffraction

Fig. 3 shows XRD patterns of samples. Apparently, the main diffraction peaks are the same as those of typical TS-1 with almost

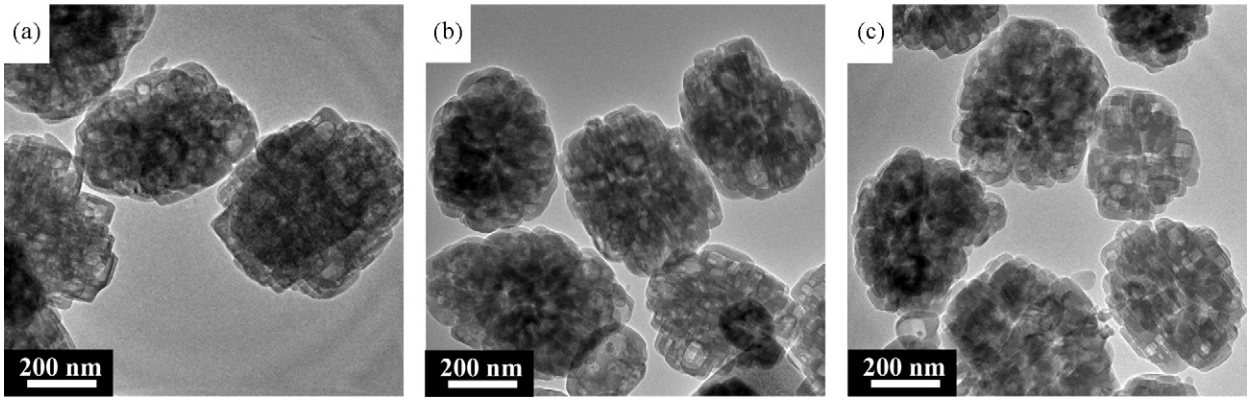

Fig. 2. TEM images of samples: (a) modified TS-1, (b) NTS-1 and (c) NTS-2.

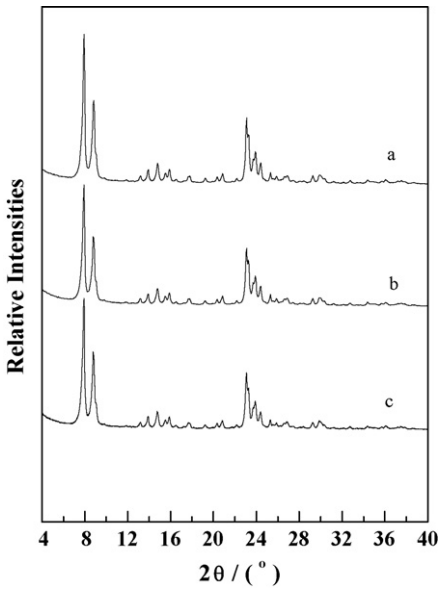

Fig. 3. XRD patterns of samples: (a) modified TS-1, (b) NTS-1 and (c) NTS-2.

the same intensities and peak resolution [15,16], indicating that the combination of Pd with the framework has almost no effect on the crystal structure. The relative crystallinities of NTS-1, NTS-2 and modified TS-1, were calculated according to the method described in Ref. [17], and the results are listed in Table 1. There are only small intensity differences among them, revealing that the combination with Pd does not affect the ordering of modified TS-1. Furthermore, there are no obvious characteristic signals of pure Pd species in XRD patterns of NTS-1 and NTS-2 (Fig. 3b and c), again suggesting the high dispersion of Pd in NTS, which is expected from the above TEM analysis [18,19].

3.5. N_2 adsorption isotherms

The N_2 adsorption isotherms of NTS samples together with that of modified TS-1 are shown in Fig. 4, and the porous parameters such as BET specific area and cumulative pore volume are listed in Table 1. Evidently, both NTS samples and modified TS-1 show the typical adsorption–desorption curves of type IV with an obvious hysteresis loop, namely, the isotherms show a very abrupt (almost linear) drop in the desorption curve, which is associated with their hollow structures [20,21]. There are no clear differences in pore structural parameters between modified TS-1 and NTS samples, implying that the effect of incorporating Pd into titanium silicate on pore structure is almost negligible, which is also in agreement with above-mentioned XRD results.

3.6. FT-IR spectra

The vibration band in IR spectra of Ti-containing zeolites is another fingerprint indicating lattice substitution of titanium sites [22]. Fig. 5 shows the FT-IR spectra of modified TS-1, NTS-1 and NTS-2. The main absorption bands are observed at 1230, 1100, 800 and 550 cm^{-1} in IR spectra of all samples, and are consistent with those of TS-1 reported in the literature [23]. It is well known that an absorption band at 960 cm^{-1} may be considered as the fingerprint of framework titanium, and commonly accepted as the characteristic of asymmetry of titanosilicate [24,25]. The characteristic "fingerprint" band is clearly detected; but for NTS-1 and NTS-2 (Fig. 5b and c), it is observed that the peak has shifted to around 970 cm^{-1}. This is likely caused by the change of the coordination structure and vibration of Ti (IV) species induced by the introduction of noble-metal. Their peak area ratios of the band at 960 cm^{-1} to that at

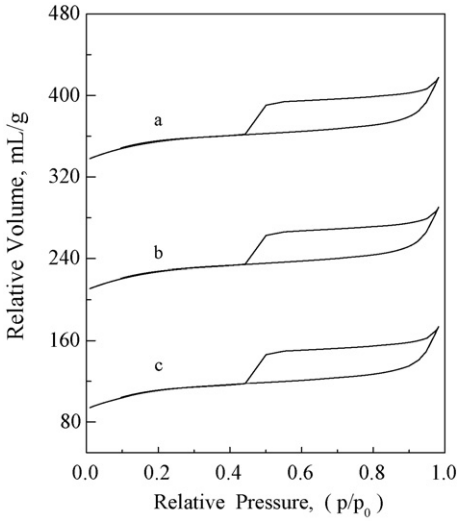

Fig. 4. N_2 adsorption/desorption isotherms of samples: (a) modified TS-1, (b) NTS-1 and (c) NTS-2.

550 cm^{-1} (I_{960}/I_{550}) in FT-IR spectra are summarized in Table 1. It can be seen that the peak area ratios of NTS-1 and NTS-2 are slightly lower than that of modified TS-1, showing that there may be an irreversible change in the framework symmetry of modified TS-1 during the noble-metal combination process [26–28].

3.7. ^{29}Si MAS NMR spectra

^{29}Si MAS NMR spectra of modified TS-1, NTS-1 and NTS-2 are shown in Fig. 6. There are peaks at $\delta = -102.8$ ppm and $\delta = -114.1$ ppm in all spectra. If the peak at $\delta = -102.8$ ppm appears, Si in samples exhibits Q_3 [$Si(OSi)_3OH$] environment, while if the peak at $\delta = -114.1$ ppm appears, Si shows Q_4 [$Si(OSi)_4$] environment [29,30]. The presence of main peak at $\delta = -114.1$ ppm together with one shoulder peak at $\delta = -102.8$ ppm indicates that there are only a few Si–OH in samples, for the intensity of shoulder peak (Q_3) is very weak compared to that of main peak (Q_4). There are no obvious changes observed from NMR spectra in chemical shift, illustrating that the combination of noble-metal with the framework of modified TS-1 has no appreciable effect on the coordination environment of Si element in NTS.

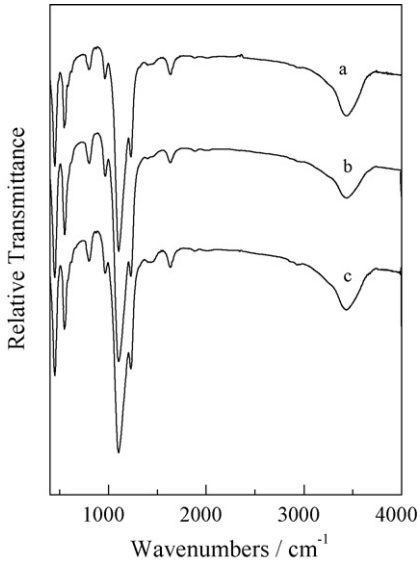

Fig. 5. FT-IR spectra of samples: (a) modified TS-1, (b) NTS-1 and (c) NTS-2.

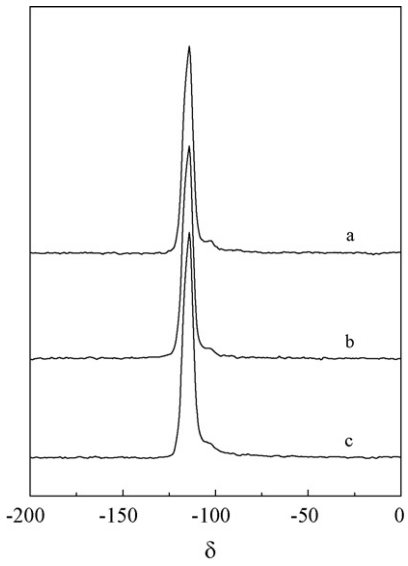

Fig. 6. ^{29}Si MAS NMR spectra of samples: (a) modified TS-1, (b) NTS-1 and (c) NTS-2.

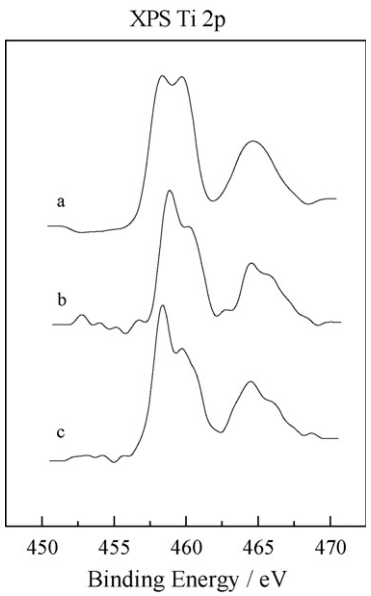

Fig. 8. XPS Ti 2p spectra of samples: (a) modified TS-1, (b) NTS-1 and (c) NTS-2.

3.8. UV–vis spectra

The intra-framework (isolated) tetrahedral Ti^{4+} species in samples were further indirectly verified by UV–vis spectra, and shown in Fig. 7. Main UV absorption bands of the samples are about at 210 and 330 nm, which show clearly the existence of intra-framework Ti^{4+} species, and extra-framework bulk titania (anatase type) [31]. An absorption band at 500 nm assigned to the absorption of noble-metal species [32] appears in UV–vis spectra of NTS-1 and NTS-2 (Fig. 7b and c). Moreover, with the increase of noble-metal content, absorption intensity of band at 500 nm was enhanced slightly, inversely proving that the band is the absorption of noble-metal species.

3.9. X-ray photoelectron spectra

XPS Ti 2p spectra of modified TS-1, NTS-1 and NTS-2 are shown in Fig. 8. All samples show two peaks at binding energy of 458.2 and 459.8 eV, which means that all the three samples have both octahedral coordination and tetrahedral coordination for titanium species [33,34], which is consistent with the analysis from above-mentioned UV–vis spectra. Pd metal shows the XPS Pd 3d peaks at 335.0 eV, PdO shows that at 336.8 eV, while NTS-1 and NTS-2 (Fig. 9a and b) show the XPS Pd 3d peaks at binding energy of 335.6 and 335.8 eV, respectively. These results indicate that the state of noble-metal in NTS is neither the one of pure simple substance nor the one of pure oxide [35], suggesting that there are interactions between noble-metal and titanium silicate, and the interactions may cause the change in electronic structure of Pd.

3.10. Catalytic results

ODS performance of NTS-1 and NTS-2 is listed in Table 1. For comparison, the results for Pd, TS-1, modified TS-1, TS-1

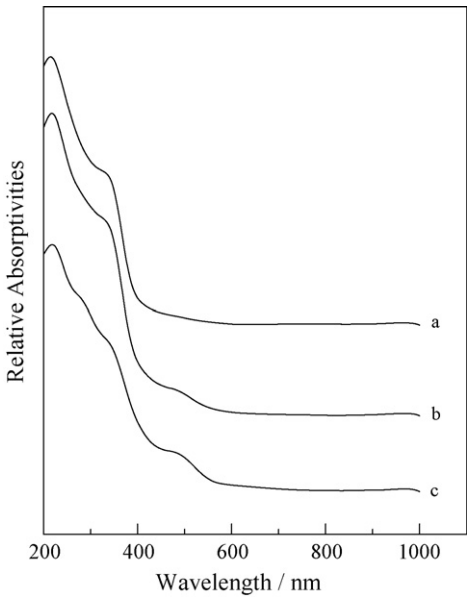

Fig. 7. UV–vis spectra of samples: (a) modified TS-1, (b) NTS-1 and (c) NTS-2.

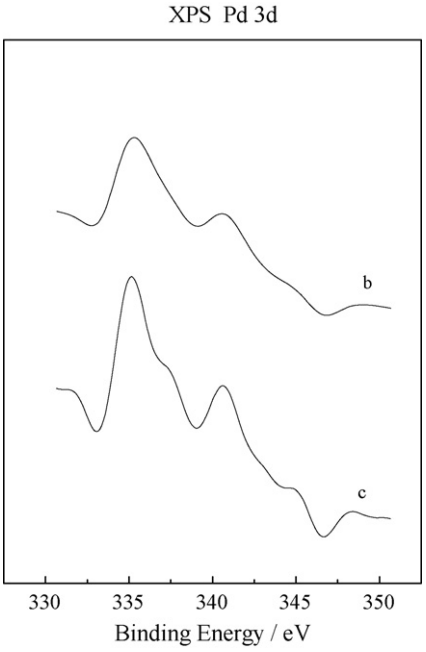

Fig. 9. XPS Pd 3d spectra of samples: (a) NTS-1 and (b) NTS-2.

impregnated with Pd (denoted by Pd/TS-1), and modified TS-1 impregnated with Pd (denoted by Pd/MTS-1) are also included in Table 1. It can be seen that Pd, TS-1 and modified TS-1 have no catalytic activities under the conditions employed for all the reaction times, while NTS samples exhibits high activity. For example, after 2 h, NTS-1 and NTS-2 give the thiophene conversion of 36% and 52%, respectively. However, the catalytic oxidation activities of Pd/TS-1 and Pd/MTS-1 (giving the thiophene conversion only at 12% and 19%, respectively) are not comparable with that. At the same time, the selectivity (the mole ratio of sulfoxide to sulfone) of NTS-1 and NTS-2 can reach 1.4 and 1.7, whereas that of Pd/TS-1 and Pd/MTS-1 was 2.0 and 1.8, respectively, meaning that there is more sulfone in the products of NTS systems than that of Pd/TS-1 and Pd/MTS-1. In other words, NTS samples have higher catalytic activities. After 6 h, the catalytic oxidation activities of NTS-1 and NTS-2 increased sharply, and gave the thiophene conversion of 75% and 87%, respectively. On the other hand, the catalytic activities of Pd/TS-1 and Pd/MTS-1 increased at a lower level, giving the thiophene conversion from 12% to 23% and from 19% to 28%, respectively. At this time, the mole ratio of sulfoxide to sulfone (selectivity) for NTS-1 and NTS-2 can reach 0.7 and 0.6, while that for Pd/TS-1 and Pd/MTS-1 was at 1.2 and 1.1, respectively. This means that more sulfone was formed with the increase of reaction time, and NTS samples are more active than that of impregnated ones (Pd/TS-1 and Pd/MTS-1) for 6 h. These results have shown that NTS shows excellent catalytic activity for the ODS of thiophene with $H_2 + O_2$ in one-step process, which may be due to its special modification treatment. Based on the above results, it can be deduced that the formation of H_2O_2 could occur over Pd species, while ODS would be over Ti species. This might explain why TS-1 and modified TS-1 (without Pd) have no catalytic activity since these materials have no Pd species and could not form H_2O_2 in situ from $H_2 + O_2$; the Pd has also no catalytic activity since it has no Ti species and could not promote thiophene oxidation. Pd/TS-1, Pd/MTS-1 and NTS samples have catalytic activities since these materials have both Pd species and Ti species; they can enhance H_2O_2 formation and thus promote thiophene oxidation. This also demonstrates that the direct thiophene oxidation process involves onsite H_2O_2 production followed by H_2O_2 reaction with thiophene to sulfoxide and sulfone [36].

4. Conclusions

NTS samples, a series of new bi-functional titanosilicates, were synthesized by combining noble-metal sources with modified TS-1 under basic conditions. Characterization results suggest that thus synthesized NTS samples with framework combining noble-metal show well ordered MFI topological and hollow structure and exhibit good catalytic activity for application in ODS with $H_2 + O_2$ in one-step process.

Acknowledgements

We are grateful for the financial support of the State Basic Research Project "973" by the Ministry of Science and Technology of People's Republic of China (2006CB202508). The authors would also like to thank Prof. Xieqing Wang, Prof. Xingtian Shu, Prof. Hong Nie, Prof. Jun Fu, Prof. Xuhong Mu and Prof. Yibin Luo in Research Institute of Petroleum Processing (RIPP), for their kind suggestions. We also thank Prof. C. Song (Pennsylvania State University, USA) for English polishing.

References

[1] F.A. Mohammad, A.M. Abdullah, E.A. Bassam, M. Gary, N.S. Mohammad, Fuel 85 (2006) 1354.
[2] X. Ma, A. Zhou, C. Song, Catal. Today 123 (2007) 276.
[3] E. Jochen, P. Wasserscheid, J. Andraeas, Green Chem. 6 (2004) 316.
[4] H. Topsoe, J. Catal. 216 (2003) 155.
[5] P.T. Vasudevan, J.L.G. Fierro, Catal. Rev. Sci. Eng. 38 (1996) 161.
[6] C. Song, X. Ma, Appl. Catal. B: Environ. 41 (2003) 207.
[7] C. Song, Catal. Today 86 (2003) 211.
[8] L.Y. Kong, G. Li, X.S. Wang, Catal. Today 93–95 (2004) 341.
[9] E. Ito, J.A.R. Veen, Catal. Today 116 (2006) 446.
[10] P.P. Olivera, E.M. Patrito, H. Selloers, Surf. Catal. 313 (1994) 25.
[11] S. Chinta, J.H. Lunsford, J. Catal. 225 (2004) 249.
[12] G. Jenzer, T. Mallat, M. Maciejewski, F. Eigenmaann, A. Baiker, Appl. Catal. A: Gen. 208 (2001) 125.
[13] R. Meiers, U. Dingerdissen, W.F. Holderich, J. Catal. 176 (1998) 376.
[14] M. Lin, X.T. Shu, X.Q. Wang, B. Zhu, US Patent 6,475,465 (5th November 2002).
[15] E. Duprey, P. Beaunier, M.-A. Springuel-Huet, F. Bozon-Verduraz, J. Fraissard, J.-M. Manoli, J.-M. Brégeault, J. Catal. 165 (1997) 22.
[16] M. Taramasso, G. Perego, B. Notari, US Patent 4,410,501 (18th October 1983).
[17] M. Lin, X.T. Shu, X.Q. Wang, B. Zhu, CN 1089279C (21st August 2002).
[18] C. Shi, R. Wang, G. Zhu, S. Qiu, J. Long, Eur. J. Inorg. Chem. 2005 (2005) 4801.
[19] C. Shi, R. Wang, G. Zhu, S. Qiu, J. Long, Eur. J. Inorg. Chem. 2006 (2006) 3054.
[20] Y. Wang, M. Lin, A. Tuel, Micropor. Mesopor. Mater. 102 (2007) 80.
[21] Y. Wang, A. Tuel, Micropor. Mesopor. Mater. 113 (2008) 286.
[22] B. Notari, Adv. Catal. 41 (1996) 253.
[23] P. Fejes, J.B. Nagy, J. Halasz, A. Oszko, Appl. Catal. A: Gen. 175 (1998) 89.
[24] C. Lamberti, S. Bordiga, A. Zecchina, A. Carati, N.F.G. Artioli, G.P.M. Salvalaggio, G.L. Marrak, J. Catal. 183 (1999) 222.
[25] G.L. Marra, G. Artioli, A.N. Fitch, M. Milanesio, C. Lamberti, Micropor. Mesopor. Mater. 40 (2000) 5.
[26] M.C. Capel-Sanchez, J.M. Campos-Martin, J.L.G. Fierro, Appl. Catal. A: Gen. 246 (2003) 69.
[27] P.F. Henry, M.T. Weller, C.C. Wilson, J. Phys. Chem. B 105 (2001) 7452.
[28] Q. Wang, L. Wang, J. Chen, Y. Wu, Z. Mi, J. Mol. Catal. A: Chem. 273 (2007) 73.
[29] R. Wang, L. Xu, L. Zhao, B. Chu, L. Hu, C. Shi, G. Zhu, S. Qiu, Micropor. Mesopor. Mater. 83 (2005) 136.
[30] W. Fan, R. Duan, T. Yokoi, P. Wu, Y. Kubota, T. Tatsumi, J. Am. Chem. Soc. 130 (2008) 10150.
[31] P. Ratnasamy, D. Srinivas, H. Knözinger, Adv. Catal. 48 (2004) 1.
[32] V.N. Shetti, P. Manikandan, D. Srinivas, P. Ratnasamy, J. Catal. 216 (2003) 461.
[33] Y. Hasegawa, A. Ayame, Catal. Today 71 (2001) 177.
[34] V. Arca, A.B. Boscoletto, N. Fracasso, L. Meda, G. Ranghino, J. Mol. Catal. A: Chem. 243 (2006) 264.
[35] W. Shen, Y. Ichihashi, M. Okumura, Catal. Lett. 64 (2000) 23.
[36] H. Song, G. Li, X. Wang, Micropor. Mesopor. Mater. 120 (2009) 346.